Citation: Molecular Therapy — Oncolytics (2016) **3,** 16034; doi:10.1038/mto.2016.34
Official journal of the American Society of Gene & Cell Therapy

www.nature.com/mto

ARTICLE

Reprogramming antitumor immunity against chemoresistant ovarian cancer by a CXCR4 antagonist-armed viral oncotherapy

Marcin P Komorowski[1,5], AJ Robert McGray[2], Agnieszka Kolakowska[1,5], Kevin Eng[3], Margaret Gil[4], Mateusz Opyrchal[4], Bogumila Litwinska[5], Michael J Nemeth[1,4], Kunle O Odunsi[2,6] and Danuta Kozbor[1]

Ovarian cancer remains the most lethal gynecologic malignancy owing to late detection, intrinsic and acquired chemoresistance, and remarkable heterogeneity. Here, we explored approaches to inhibit metastatic growth of murine and human ovarian tumor variants resistant to paclitaxel and carboplatin by oncolytic vaccinia virus expressing a CXCR4 antagonist to target the CXCL12 chemokine/CXCR4 receptor signaling axis alone or in combination with doxorubicin. The resistant variants exhibited augmented expression of the hyaluronan receptor CD44 and CXCR4 along with elevated Akt and ERK1/2 activation and displayed an increased susceptibility to viral infection compared with the parental counterparts. The infected cultures were more sensitive to doxorubicin-mediated killing both *in vitro* and in tumor-challenged mice. Mechanistically, the combination treatment increased apoptosis and phagocytosis of tumor material by dendritic cells associated with induction of antitumor immunity. Targeting syngeneic tumors with this regimen increased intratumoral infiltration of antitumor CD8$^+$ T cells. This was further enhanced by reducing the immunosuppressive network by the virally-delivered CXCR4 antagonist, which augmented antitumor immune responses and led to tumor-free survival. Our results define novel strategies for treatment of drug-resistant ovarian cancer that increase immunogenic cell death and reverse the immunosuppressive tumor microenvironment, culminating in antitumor immune responses that control metastatic tumor growth.

Molecular Therapy — Oncolytics (2016) **3**, 16034; doi:10.1038/mto.2016.34; published online 14 December 2016

INTRODUCTION

The key biological processes leading to the formation of highly aggressive and metastatic ovarian cancer recurrences are not clearly understood, stressing the need for both an improved understanding of disease resistance as well as effective treatment options for relapsed cancers that are both phenotypically and biologically heterogeneous.[1–3] Individual ovarian tumors show distinct subareas of proliferation and differentiation, often with regions undergoing epithelial-mesenchymal transition, where cancer initiating cells (CICs) have the capacity to indefinitely self-renew and sustain tumor growth.[4] It is thought that CD44$^+$ CICs are able to survive conventional chemotherapies, giving rise to recurrent tumors that are more resistant and aggressive.[4,5] The presence of CD44$^+$ ovarian cancer cells has been correlated with chemoresistance to a front-line treatment with paclitaxel (PTX) and carboplatin (CBDCA) associated with induction of molecular modifications in the pre-existing CICs.[6,7] Given the heterogeneous nature of the ovarian tumor microenvironment (TME), therapeutic approaches that act across the different subtypes of epithelial ovarian cancer and target both chemoresistant cancer cells and the TME that promotes tumor growth would be of clear benefit. Additionally, as the presence of tumor-infiltrating CD8$^+$ T lymphocytes and a high CD8$^+$/regulatory T cell (Treg) ratio are associated with improved survival in patients with ovarian tumors,[8–10] it is imperative that newly developed treatments also initiate or enhance antitumor immune responses that promote durable tumor control.

Oncolytic viruses (OVs) including vaccinia (OVV) mediate anticancer effects by both direct oncolysis and stimulation of innate immune responses through production of damage-associated molecular patterns and the presence of virus-derived pathogen-associated molecular patterns,[11,12] leading to increased Type 1 IFN production.[13,14] Additionally, OVV-mediated oncolysis may facilitate the direct acquisition of tumor-derived antigens by host antigen-presenting cells within the TME, thereby leading to improved T cell priming as well as coordination of the effector phase of antitumor immune responses. A currently initiated clinical trials of GL-ONC1 vaccinia virus against high-grade serous, endometrioid, or clear-cell ovarian cancer which includes: (i) platinum-resistant (recurrence or progression in < 6 months) or (ii) platinum-refractory (progression while on platinum-based therapy) (NCT02759588), emphasizes the unmet medical need to develop new therapies that are effective in patients that do not respond to chemotherapy. Furthermore, such

[1]Department of Immunology, Roswell Park Cancer Institute, Buffalo, New York, USA; [2]Center for Immunotherapy, Roswell Park Cancer Institute, Buffalo, New York, USA; [3]Department of Biostatistics and Bioinformatics, Roswell Park Cancer Institute, Buffalo, New York, USA; [4]Department of Medicine, Roswell Park Cancer Institute, Buffalo, New York, USA; [5]Department of Virology, National Institute of Public Health-National Institute of Hygiene, Warsaw, Poland; [6]Department of Gynecologic Oncology, Roswell Park Cancer Institute, Buffalo, New York, USA. Correspondence: D Kozbor (danuta.kozbor@roswellpark.org)
Received 25 August 2016; accepted 3 November 2016

studies are vital to understanding the mechanisms of action of OVV-based treatments that may, in turn, guide the development of rational combination therapies for future clinical trials.

In addition to a direct effect of oncolytic virotherapy on drug-resistant malignant cells, the interaction of cancer cells with their microenvironment, which protects the malignant cells from genotoxic stresses such as chemotherapy, is an attractive target to improve anticancer treatment. Several lines of evidence indicate that activation of the chemokine CXCL12 pathway increases tumor resistance to both conventional therapies and biological agents by: (i) directly promoting cancer cell survival, invasion, and the cancer stem and/or tumor-initiating cell phenotype; (ii) recruiting "distal stroma" (*i.e.*, myeloid BM-derived cells) to indirectly facilitate tumor recurrence and metastasis; and (iii) promoting angiogenesis directly or in a paracrine manner.[15,16] These findings suggest that anticancer efficacy can be greatly improved by inhibiting the CXCL12/CXCR4 axis prompting us to test the feasibility of targeting PTX- and CBDCA-resistant variants of murine ID8-R and human CAOV2-R ovarian cancer cells using the armed OVV ((*i.e.*, expressing the CXCR4 antagonist in-frame with the Fc portion of murine IgG2a (OVV-CXCR4-A-Fc)) alone or in combination with doxorubicin (DOX). The latter drug was chosen for the combination treatment because the pegylated liposomal doxorubicin (PLD) has become a major component in the routine management of epithelial ovarian cancer used for treatment of platinum-resistant ovarian cancer.[17] Furthermore, as T-cell exclusion from tumors is associated with low expression levels of Type 1 IFN associated genes,[18] increased expression of these genes during OVV infection may improve the impact of responses to anthracycline (*i.e.*, DOX)-based chemotherapy,[19] and could potentiate the antitumor immune response by enhancing local infiltration of inflammatory cells following infection. Although DOX-based chemotherapy has been previously showed to synergize with oncolytic adenovirus against soft-tissue sarcomas in hamsters, the virus did not provide a clear advantage over DOX alone with regards to *in vivo* efficacy perhaps because the hamster model is only semipermissive to human adenovirus.[20] Using different delivery modes of OVV and DOX, we show that OVV delivered prior to DOX treatment elicited a multifaceted response resulting in a synergistic increase involving direct oncolysis of the resistant variants, a decrease in intratumoral recruitment of immunosuppressive elements, and stimulation of antitumor immunity that led to curative inhibition of tumor growth. These outcomes were most apparent following treatment with OVV-CXCR4-A-Fc, demonstrating that armed oncolytic virotherapy can further modulate the antitumor immune response.

RESULTS

Increased susceptibility of PTX- and CBDCA-resistant ovarian tumor cells to vaccinia virus infection

To investigate strategies for effective killing of drug-resistant ovarian tumor cell variants, we used PTX- and CBDCA-resistant murine ID8-R and human CAOV2-R ovarian tumors selected for drug resistance and maintained in media supplemented with PTX (59 nmol/l) and CBDCA (2.6 µmol/l). At these drug concentrations, the resistant variants exhibited small decreases in growth rates compared with their parental tumor cells (Supplementary Figure S1) and expressed over twofold higher levels of CD44 antigen in both ID8 (mean fluorescence intensity (MFI): 30±4 versus 12±2) and CAOV2 (MFI: 225±15 versus 126±13) when compared with parental cell cultures (Figure 1a). Expression of the CXCR4 receptor was also elevated in the resistant compared with the parental variants of ID8 (MFI: 24±3 versus 11±1) and CAOV2 (MFI: 36±5 versus 16±2) cells (Figure 1b). Consistent with the increased CD44 and CXCR4 expression and their association with the ovarian CIC-like phenotype,[21,22] ID8-R and CAOV2-R variants exhibited higher tumorigenicity when injected in exponentially smaller numbers intraperitoneally (i.p.) into syngeneic or SCID mice, respectively. As shown in Table 1, a minimum of 5×10^6 ID8-P cells was required to consistently initiate i.p. tumor growth in all inoculated mice within a 8-week period, whereas injection of 4% of that number formed ID8-R tumors within a much shorter period of time. Similar results were obtained with the parental and CAOV2-R tumors in SCID mice where the number of resistant cells necessary to form i.p. tumors was only 40% of the required number of parental cells (Table 1).

Infection of the resistant variants with oncolytic vaccinia virus expressing the enhanced green fluorescence protein (OVV-EGFP) at multiplicity of infection (MOI) of 1, showed over twofold increase in the number of $EGFP^+$ cells 24 hours after infection (Figure 1c,d) and resulted in higher viral titers than those recovered in the parental cultures (Figure 1e, $P \leq 0.01$). In line with evidence that Akt[23] and MEK/ERK[24] pathways augment vaccinia replication,[25] Western blotting of ID8-R cellular lysates revealed 2- and sixfold higher Akt phosphorylation levels at S473 and T308 as well as sixfold higher ERK1/2 phosphorylation compared with the parental cells (Figure 1f). In CAOV2-R variants, the level of Akt(S473-P) showed small increases in contrast to 26-fold higher expression of pERK1/2 compared with parental cells (Figure 1f).

Cytopathic effects of OVV and DOX combination treatments

Next, we examined whether cytopathic effects of vaccinia virus could be augmented by DOX treatment using a 72-hour cell viability assay with serial dilutions of OVV-EGFP and DOX added alone or in combination to the parental and drug-resistant variants of ID8 and CAOV2 cells. As expected based on the higher infection and replication rates of vaccinia, ID8-R variants were more susceptible to the lytic effect of vaccinia than the parental cells based on fivefold less virus needed to achieve 50% killing (EC_{50}) (Figure 2a, left panel). Similarly, CAOV2-R cells were fourfold more sensitive to the vaccinia-mediated killing than the parental cells (Figure 2a, right panel). However, the sensitivity profile of drug-resistant variants to DOX-mediated killing was opposite to that of the virus. For example, the IC_{50} values for ID8-R cells were ~10-fold higher compared with the parental cells ($P = 0.0003$; Figure 2b, left panel). The increased resistance to DOX was also evident in CAOV2-R cells (Figure 2b, right panel) with threefold differences in the IC_{50} values between the resistant and parental cells ($P = 0.04$). The increased cross-resistance of ID8-R and CAOV2-R variants compared with their parental counterparts could be attributed to higher proportions of the "side population" (SP) cells in the resistant variants whose intrinsic dye efflux export many cytotoxic drugs and enhance resistance to chemotherapeutic agents.[26,27] Staining with fluorescence dye Hoechst 33342 showed threefold to fivefold higher proportion of $Hoechst^{low}$ SP cells in ID8-R and CAOV2-R cells compared with the parental cells (range: 0.3–1.5% versus 2.9–5.6%; Supplementary Figure S2a). Culturing the tumor cells in the presence of DOX (3 µmol/l) showed that the initial growth rates of the resistant variants in the presence of DOX were lower compared with those in PTX (59 nmol/l) and CBDCA (2.6 µmol/l) with over 90% dead cells after a 1-week period (Supplementary Figure S2b,c), indicating that increases in SP cells were not adequate to afford a durable survival advantage in the presence of DOX.

Because both the parental and the resistant cell lines were susceptible to the cytopathic effect of OVV and DOX, albeit with different

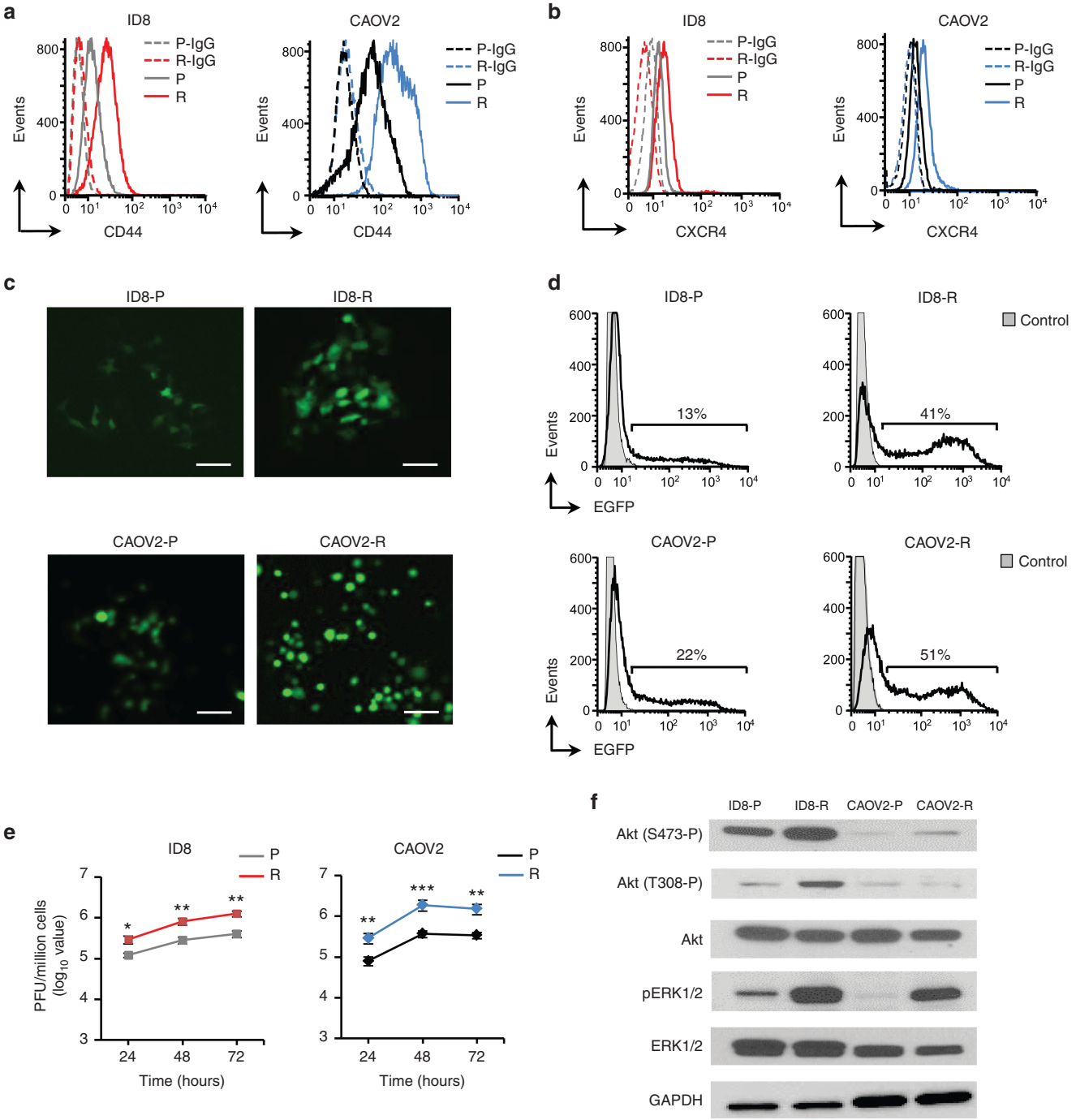

Figure 1 Phenotypic characterization of ID8-R and CAOV2-R ovarian tumor cells and their parental counterparts. Flow cytometry analysis of CD44 (**a**) and CXCR4 (**b**) expression in parental and drug-resistant variants was performed on single-cell suspensions with specific mAbs. Background staining was assessed using isotype control Abs. Data are from one representative experiment of three performed. (**c**) Susceptibility of ID8-R and CAOV2-R to vaccinia virus infection. The parental and drug-resistant tumor cells were cultured as a monolayer before infection with OVV-EGFP (MOI = 1). The expression of EGFP in infected cells was examined under an immunofluorescence microscope 24 hours later. Scale bars = 25 µm. One representative experiment of three performed is shown. (**d**) The number of EGFP-expressing cells in each culture was determined by examining single-cell suspensions 24 hours after infection by flow cytometry analysis. Background staining depicts uninfected controls. One representative experiment of four independent experiments performed is shown. (**e**) Replication of OVV-EGFP in different cultures was determined by titrating viral particles released from the infected cells at different time points by plaque assays in CV-1 cell monolayers. Results are presented as the mean of plaque forming units (PFU)/million cells ± SD of three independent experiments performed in duplicate. **P* < 0.05, ***P* < 0.01, and ****P* < 0.001. (**f**) Phosphorylation levels of Akt and ERK1/2 in tumor cells were determined by Western blotting with antiphospho-Akt(S473-P), antiphospho-Akt(T308-P) and antiphospho-ERK1/2 (Thr202/Tyr204) Abs. Antitotal Akt and antitotal ERK1/2 Abs were used as internal controls and anti-GAPDH Ab was used as a loading control. Bands were developed with HRP-labeled secondary Abs followed by Clarity Western ECL detection system. Representative blot from one experiment out of three performed is shown. GAPDH, glyceraldehyde 3-phosphate dehydrogenase; MOI, multiplicity of infection; OVV-EGFP, oncolytic vaccinia virus expressing the enhanced green fluorescence protein.

levels of efficacy, we next asked whether these two therapies could potentially synergize to further enhance tumor cell killing. To determine whether the sequence of the treatments was important, the parental and resistant cells were treated with different concentrations of DOX added 12 hours after, simultaneously, or 12 hours before the virus used at the EC_{50} titers. As shown in Figure 2c,d (left panel), treatment of both variants with vaccinia for 12 hours prior to DOX revealed the highest cytopathic effect compared with monotherapy treatments. However, the effect was less prominent in the parental cells than in the resistant variants reflecting the low susceptibility of these cells to vaccinia infection and high sensitivity to DOX. On the other hand, ~80% of cell death was achieved in both ID8-R and CAOV2-R cultures even at concentrations of DOX that had small cytopathic effects when used alone, indicating a synergistic interaction between these two agents in cell-mediated killing of resistant cells. The simultaneous treatment with both agents appeared to be less than additive (Figure 2c,d, middle panel), whereas treatment of tumor cells with DOX prior to infection inhibited viral killing (Figure 2c,d, right panel). Thus, the over fivefold difference in cytopathic effects between the most and least effective combination treatments (*e.g.*, OVV followed by DOX versus DOX followed by OVV) in the resistant cultures compared with only twofold difference in the parental counterparts suggest that the chemosensitivity profile of tumor cells affects efficacy of the OVV and DOX delivery. The reduced viral replication in the presence of DOX is consistent with threefold and 10-fold decreases in viral titers in CAOV2-R and ID8-R cultures treated with DOX 12 hours following vaccinia infection compared with virus infection alone (Supplementary Figure S3a). Also, Western blotting of the infected and DOX-treated cultures with vaccinia-specific serum revealed lower expression of viral antigens compared with cells infected in the absence of the drug with more prominent differences in ID8-R cells (Supplementary Figure S3b).

Table 1 *In vivo* tumorigenicity of parental and drug-resistant ID8 and CAOV2 cells

Cell type[a]	*Injection route*	*Mice*	*Cell dose*[b]	*Tumor formation*[c]	*Latency days*[d]
ID8-P	i.p.	C57BL/6	5×10^6	5/5	60.4 ± 4.2
ID8-P	i.p.	C57BL/6	1×10^6	1/6	72
ID8-P	i.p.	C57BL/6	5×10^5	0/5	NA[e]
ID8-R	i.p.	C57BL/6	1×10^6	6/6	24.1 ± 4.5
ID8-R	i.p.	C57BL/6	2×10^5	8/8	29.4 ± 3.6
ID8-R	i.p.	C57BL/6	1×10^5	4/6	38.3 ± 3.1
ID8-R	s.c.	C57BL/6	5×10^4	0/5	NA
CAOV2-P	i.p.	SCID	5×10^6	5/5	37.4 ± 4.8
CAOV2-P	i.p.	SCID	3×10^6	3/6	59.8 ± 3.7
CAOV2-P	i.p.	SCID	1×10^6	1/5	82
CAOV2-R	i.p.	SCID	2×10^6	8/8	29.2 ± 6.1
CAOV2-R	i.p.	SCID	1×10^6	4/5	46.3 ± 9.2
CAOV2-R	i.p.	SCID	5×10^5	1/5	73

i.p., intraperitoneal; s.c., subcutaneous.
[a]Parental and PTX- and CBDCA-resistant ID8 and CAOV2 tumor cells were injected i.p. at different numbers into syngeneic C57BL/6 or SCID mice and monitored for tumor growth. [b]No. of cells/injection. [c]No. of tumors/no. of injections. [d]Time from injection to the first appearance of ascites. Results are presented as mean ± SD. [e]NA, not applicable.

Protection against ID8-R metastases by single and combination treatment with OVV and PLD

To effectively test the multiple mechanisms of synergy between OVV and DOX treatments, we next examined whether the effect of DOX on tumor cell killing *in vitro* could be translated to the orthotopic growth of ID8-R and CAOV2-R tumors in syngeneic and SCID mice, respectively. For the *in vivo* experiments, DOX was replaced with its pegylated liposomal form known as PLD whereas OVV-EGFP was replaced with the Fc portion of murine IgG2-expressing vaccinia virus (OVV-Fc) because the immune response against EGFP in infected mice could alter the treatment efficacy.[28] Both OVV-EGFP and OVV-Fc have similar effects on tumor cell killing (Supplementary Figure S4). ID8-R cells (2×10^5) were injected i.p. into syngeneic C57BL/6 mice and treated 10 days later with PLD or OVV-Fc delivered as single agents or in combination. PLD (10 mg/kg) was delivered i.v. whereas vaccinia viruses (10^8 plaque forming units (PFU)/injection) were delivered i.p. Because the kinetics of vaccinia virus spreading infection in tumor-bearing mice differs from that in cell cultures, with the peak and cessation of viral replication occurring on days 4 and 8, respectively,[29,30] we used an 8-day interval period between OVV-Fc and PLD treatments to ensure that PLD did not interfere with vaccinia replication (Figure 3a). Progression of tumor growth, quantified by bioluminescence imaging (Figure 3a,b) revealed rapid tumor progression in control mice that were killed within 5 weeks after tumor challenge (Figure 3c). PLD treatment alone was not effective in controlling tumor spread and extended survival by ~1 week compared with the control mice. The antitumor efficacy of OVV-Fc or OVV-Fc delivered after PDL reduced progression of tumor growth by 2 weeks after which period tumor growth continued at a rate similar to that in the control mice. Treatment with OVV-Fc followed by PLD had more potent antitumor activities extending the slower rate of tumor growth and survival for ~ 2 and 4 weeks compared with mice treated with the virus only ($P < 0.001$) or virus delivered together with PLD ($P = 0.002$; Figure 3c). Interestingly, the antitumor effect of OVV-Fc and PLD treatments delivered together was similar to that achieved when PLD was delivered 12 hours after the viral infection (Supplementary Figure S5), highlighting that a longer time interval between delivery of the two treatments is required to achieve optimal therapeutic benefit.

Immune responses against dying cells after OVV followed by DOX treatment are associated with increased apoptosis and phagocytosis of tumor cells by dendritic cells (DCs)

To explore cellular mechanisms involved in the synergistic killing of the drug-resistant tumor cells with vaccinia followed by DOX treatment we investigated the induction of tumor cell death by each treatment alone or in combination. The induction of apoptosis and necrosis was investigated in 24 hours cultures of ID8-R tumor cells treated with vaccinia virus at MOI of 1, which roughly corresponds to the EC_{50} titer, or DOX (1 µmol/l) alone or in combination. In the combination treatment, OVV was added 12 hours before DOX and induction of apoptosis/necrosis was analyzed by flow cytometry with Annexin V-FITC and LIVE/DEAD fixable violet. While DOX or vaccinia alone induced apoptosis or necrosis in ~20% of cells, the combination treatment significantly increased early apoptosis (Annexin V^+ and LIVE/DEAD fixable $violet^-$) compared with cultures treated with OVV-Fc or DOX only (Figure 4a,b; $P = 0.0008$ and $P = 0.009$). Late apoptosis/necrosis (Annexin $V^{+/-}$ and LIVE/DEAD fixable $violet^+$) was increased to a

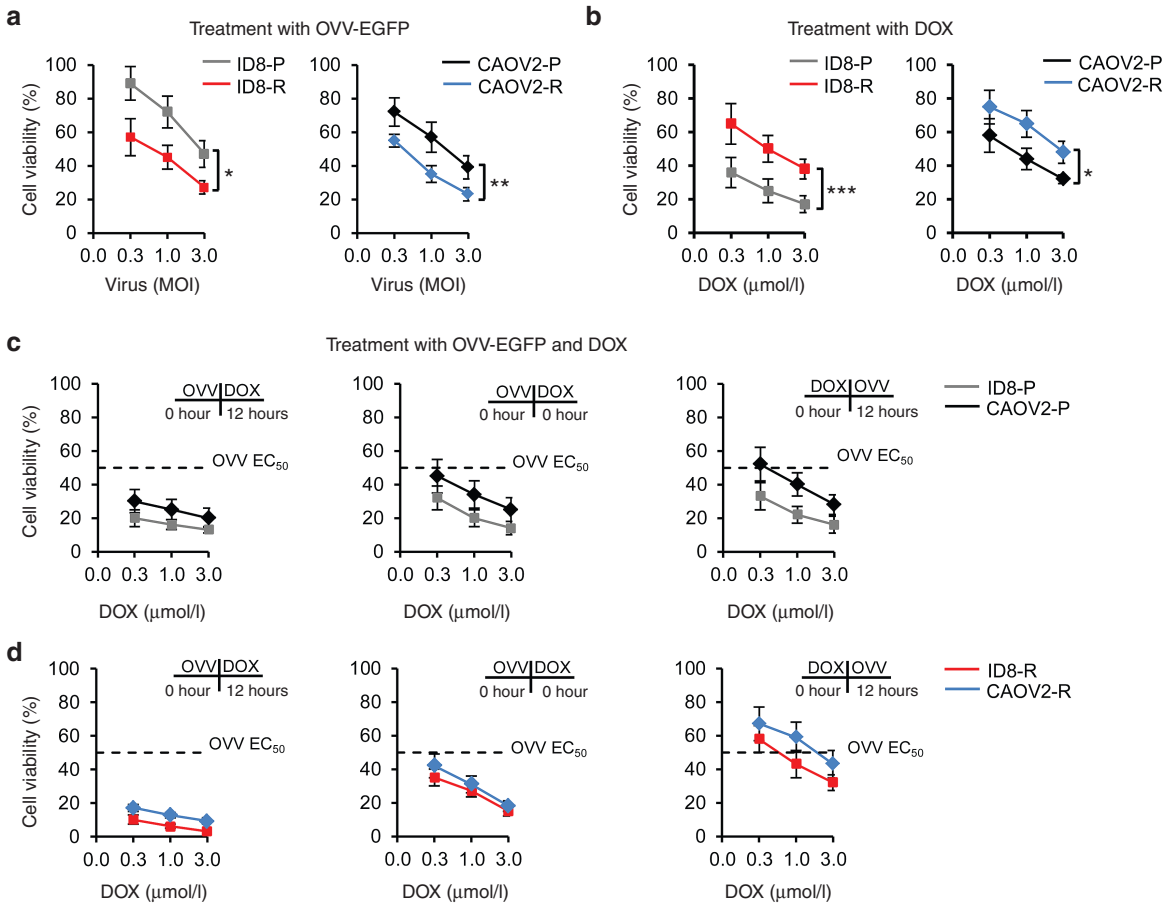

Figure 2 Cytotoxicity of vaccinia virus and DOX used alone or in combination. Cells plated in 96-well plates were treated with serial dilutions of OVV-EGFP (**a**) or DOX (**b**). Cell survival was determined after 72 hours by 3-(4,5-Dimethylthiazol-2-yl)-2, 5-diphenyltetrazolium bromide (MTT) assay and calculated using the following formula: % cell survival = (absorbance value of treated cells/absorbance value of untreated control cells) × 100%. Each data point was generated from triplicate samples repeated twice. Results are presented as mean ± SD. *$P < 0.05$, **$P < 0.01$, and ***$P < 0.001$. The effect of combination treatments of vaccinia virus and DOX against parental (**c**) and resistant (**d**) ID8 and CAOV2 tumor cells. The virus (EC_{50}) was added 12 hours before treatment with serial dilutions of DOX (left panel), together with DOX (middle panel), or 12 hours after DOX (right panel). Cell survival was determined after 72 hours by MTT assay. Each data point was generated from triplicate samples repeated twice. Results are presented as mean ± SD. DOX, doxorubicin; OVV-EGFP, oncolytic vaccinia virus expressing the enhanced green fluorescence protein.

lesser extent, altogether reducing the number of viable cells by 70%. Similar results were observed with CAOV2-R cells (Supplementary Figure S6). To address the possibility that the viral infection produced a bystander effect by releasing factors capable of sensitizing ID8-R tumor cells to DOX, culture supernatants from uninfected or 24 h-infected ID8-R cultures were filtered and treated with UV and psoralen to remove any infectious virus prior to adding to fresh uninfected cells. OVV treatment-conditioned and virus-negative (CVN) medium, when added to uninfected ID8-R cultures, induced modest increases in early apoptosis but significantly enhanced the effect of DOX (Figure 4c; $P = 0.03$). This effect could be attributed to IFN-β production which was detected in the CVN medium by enzyme-linked immunosorbent assay (ELISA) (86 ± 13 pg/ml). Treatment with IFN-β blocking antibody reduced the apoptotic activity of CVN medium alone or when combined with DOX, by as much as 80% (Figure 4c). This finding supports the previously reported ability of Type 1 IFN to enhance anthracycline-based chemotherapy.[19] The viral treatment of ID8-R or CAOV2-R cells followed by DOX was also effective in inducing surface exposure of calreticulin (ecto-CRT) (Figure 4d) known to enhance immunogenicity of cancer cell death.[31]

In view of the established role of surface CRT as an "eat me" signal,[32,33] we investigated the phagocytosis of the treated tumor cells by BM-derived DCs, which is stringently required for mounting immune response against dying tumor cells.[34] As shown in Figure 4e, ID8-R tumor cells that received the combination of OVV and DOX were over threefold more efficiently phagocytosed by DCs compared with either agent alone. To test the immunogenicity of tumor cells treated with single agent or combination therapies as vaccines, ID8-R cells exposed to OVV-Fc or DOX alone or in combination were injected into one flank of immunocompetent C57BL/6 mice. The mice were then challenged with live ID8-R cells injected into the opposite flank 8 days later. Protection against tumor growth was interpreted as a sign of successful vaccination and induction of antitumor immunity (Figure 4f), since such protection was not observed in SCID mice (data not shown). These data suggest that the combination of OVV and DOX led to upregulation of factors associated with immunogenic cell death (ICD) that could potentiate the benefits of direct tumor cell killing by augmenting the induction of antitumor immunity.

Inhibition of i.p. dissemination of ID8-R tumor and improved overall survival by OVV-CXCR4 followed by PLD treatment

Although the combination treatment with OVV-Fc followed by PLD significantly inhibited growth of ID8-R tumor *in vivo* compared

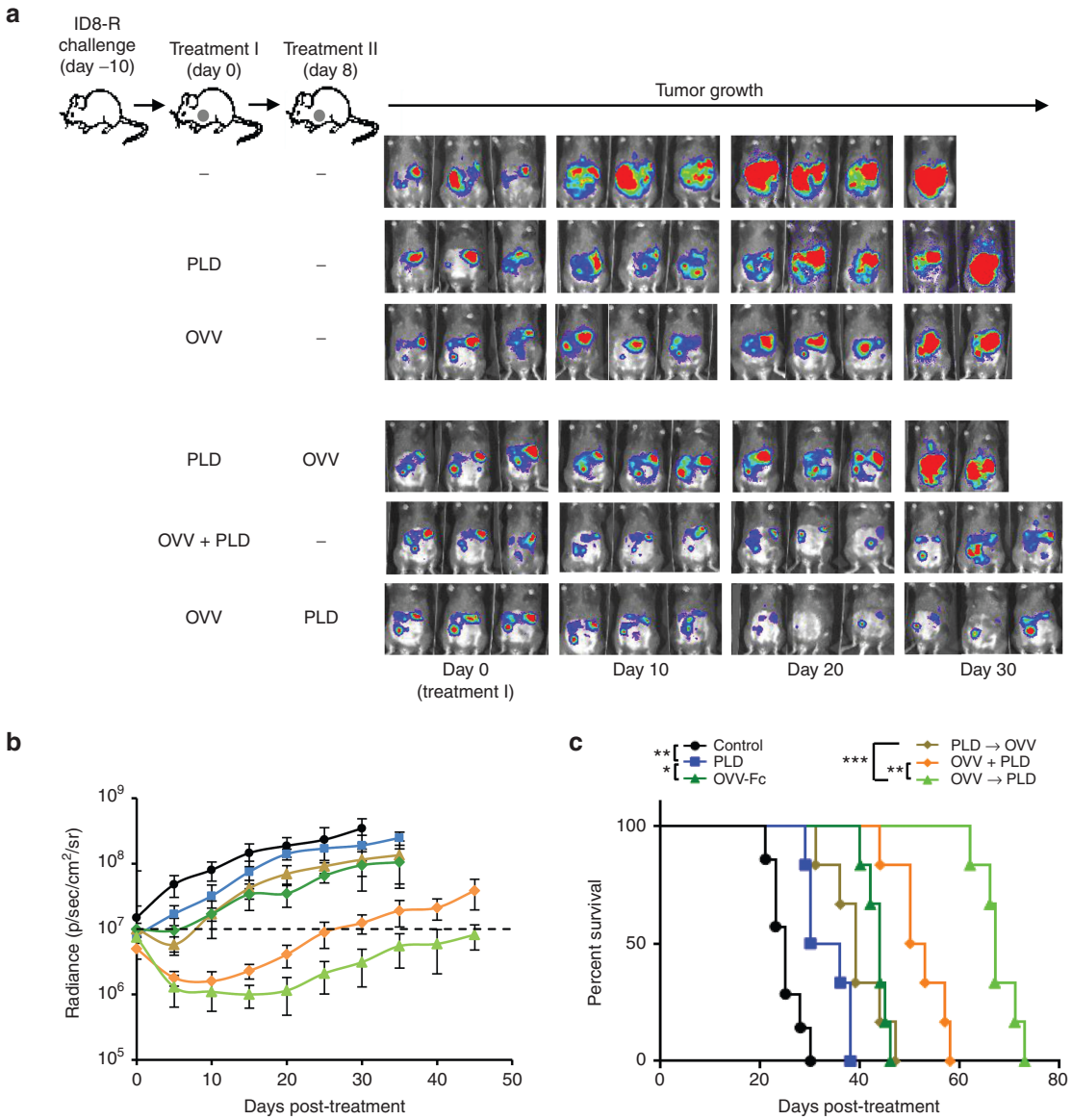

Figure 3 Efficacy of oncolytic virotherapy and PLD treatment used alone and in combination against i.p. growth of ID8-R in syngeneic mice. (**a**) C57BL/6 mice ($n = 6$ –10) were injected i.p. with 2×10^5 ID8-R cells. Oncolytic virotherapy with OVV-Fc (10^8 PFU delivered i.p.) alone or in combination with PLD (10 mg/kg delivered i.v.) was initiated 10 days later. In parallel experiments, tumor-bearing mice were treated with PLD, or PLD was delivered to tumor bearing mice 8 days before or after virotherapy treatment. Control mice were treated with PBS. (**b**) Tumor progression was monitored by bioluminescence imaging using the Xenogen IVIS Imaging System. Data points represent mean ± SD. (**c**) Survival was defined as the point at which mice were killed because of extensive tumor burden. Kaplan–Meier survival plots were prepared and significance was determined using the log-rank method. *$P < 0.05$, **$P < 0.01$, ***$P < 0.001$. OVV, oncolytic vaccinia virus; PLD, pegylated liposomal doxorubicin; PBS, phosphate buffered saline; PFU, plaque forming units; SD, standard deviation.

with single modality treatments, it did not provide permanent regression. This, together with the accumulating evidence that the chemokine CXCL12 pathway increases tumor resistance to both conventional therapies and biological agents,[15,16,29,35,36] prompted us to employ an armed virus expressing a CXCR4 antagonist. The antagonist, developed based on the CTCE-9908 peptide analog of CXCL12 (refs. [37,38]) and expressed in the context of murine (Fc) or human (hFc) fragment of IgG,[29] is capable of binding and inducing apoptosis in ~30% of CXCR4-expressing ID8-R and CAOV2-R cells (Figure 5a and Supplementary Figure S7). Because previous studies have shown efficacy of the CXCR4 antagonist in murine models of metastatic breast and ovarian tumors,[29,36,39] we next examined whether a targeted delivery of CXCR4-A-Fc by the virus followed by PLD would lead to improve overall survival of syngeneic mice challenged i.p. with ID8-R tumors. OVV-Fc was used as a control for these studies. Progression of tumor growth quantified by bioluminescence imaging revealed that although each monotherapy decreased tumor growth and metastatic dissemination compared with untreated controls, no single agent treatments alone eliminated tumors (Figure 5b,c). Treatment with OVV-Fc followed by PLD had more potent antitumor activities extending the slower rate of tumor growth and survival for almost 4 weeks compared with mice treated with the virus or PLD only ($P < 0.006$). However, oncolytic virotherapy using the armed OVV-CXCR4-A-Fc virus followed by PLD was most effective in inhibiting tumor growth resulting in tumor-free survival in ~20% of ID8-R tumor-bearing mice (Figure

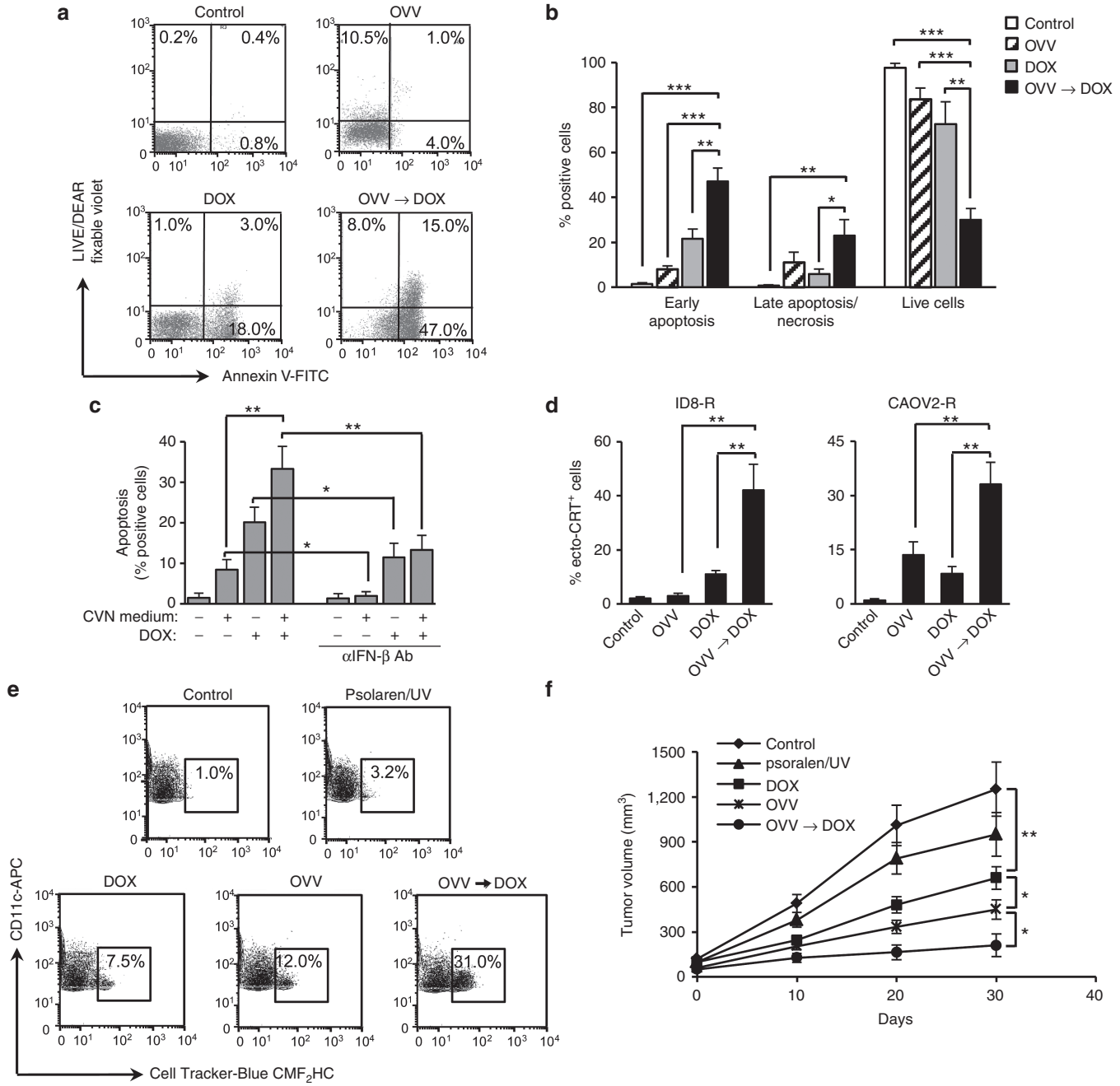

Figure 4 Virally-induced IFN-β expression augments DOX-induced apoptosis associated with increased surface exposure of surface CRT, phagocytosis of tumor cell debris by BM-derived DCs, and immunogenicity. Cell death in ID8-R tumor cells treated with OVV-Fc (MOI = 1), DOX (1 µmol/l) or OVV-Fc followed by DOX (12 hours after infection) was determined by staining with Annexin V-FITC and LIVE/DEAD fixable violet to measure the induction of early apoptosis (Annexin V^+/LIVE/DEAD fixable $violet^-$) and late apoptosis/necrosis (Annexin $V^{+/-}$/LIVE/DEAD fixable $violet^+$) by flow cytometry 24 hours later. (**a**) One representative experiment of three independent experiments performed is shown. (**b**) Results are presented as the mean ± SD of three independent experiments. $^*P < 0.05$, $^{**}P < 0.01$, $^{***}P < 0.001$. (**c**) Culture supernatants were collected from OVV-Fc-infected ID8-R cells, filtered and treated with UV and psolaren (10 µg/ml). Culture supernatants collected from uninfected cells served as controls. The CVN media were added to uninfected ID8-R cultures alone or in combination with DOX and analyzed for induction of early apoptosis. The induction of early apoptosis in cultures treated with the CVN supernatant and DOX alone or in combination was inhibited by IFN-β blocking antibody (0.5 µg/ml). Data points represent mean ± SD of three independent experiments. $^*P < 0.05$, $^{**}P < 0.01$. (**d**) Surface exposure of CRT in ID8-R (left panel) and CAOV2-R (right panel) cultures untreated or treated with OVV-Fc, DOX, or OVV-Fc and DOX combination was determined by flow cytometry after staining with an anti-CRT Ab or an isotype control 24 hours after treatments. Results are presented as mean ± SD of four independent experiments. $^{**}P < 0.01$. (**e**) Phagocytosis of cell-tracker-blue CMF_2HC-labeled tumor cells treated with OVV-Fc, DOX, or OVV-Fc and DOX combination by DCs was measured after 12 hours by flow cytometry. All tumor cell cultures infected with vaccinia virus were treated with UV and psolaren to eliminate the virus before combining with DCs. Tumor cells receiving UV and psolaren treatment were included as additional controls. The percentages of CD11c-expressing DCs taking up tumor cells are indicated. One representative experiment of three independent experiments performed is shown. (**f**) *In vivo* anticancer vaccination. ID8-R cells cultured as described above were injected in one flank of five C57BL/6 mice per group. This was followed by injection of live tumor cells into the opposite flank 8 days later. Tumor growth was monitored by measuring s.c. tumor growth with microcaliper until control mice were killed due to extensive tumor burden. Results are presented as mean ± SD of five independent experiments. $^*P < 0.05$, $^{**}P < 0.01$. BM, bone marrow; CVN, OVV treatment-conditioned and virus-negative; DOX, doxorubicin; IFN, interferon; MOI, multiplicity of infection; OVV, oncolytic vaccinia virus; SD, standard deviation.

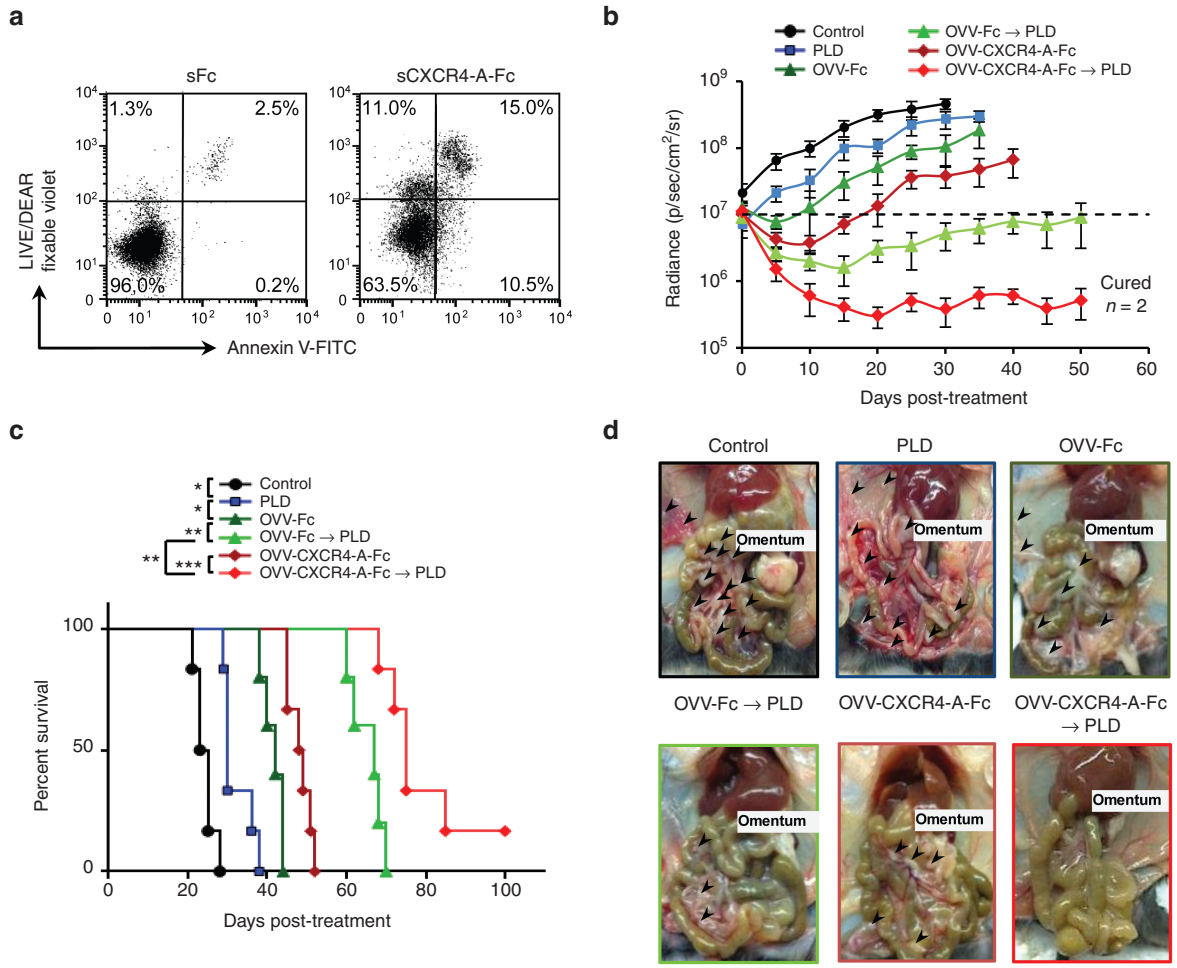

Figure 5 Effect of the CXCR4-A-Fc fusion protein on ID8-R tumor growth. (**a**) Cell death in ID8-R tumor cells treated with soluble CXCR4-A-Fc fusion protein (100 µg/ml) for 24 hours was determined by staining with Annexin V-FITC and LIVE/DEAD fixable violet. Tumor cells treated with soluble Fc fragment of mouse IgG2a serve as controls. One representative experiment of three independent experiments performed is shown. (**b**) C57BL/6 mice ($n = 8 - 10$) were injected i.p. with 2×10^5 ID8-R cells. Oncolytic virotherapy with OVV-CXCR4-A-Fc or OVV-Fc (10^8 PFU delivered i.p.) was initiated 10 days later. In parallel experiments, tumor-bearing mice were treated with PLD (10 mg/kg) delivered i.v. or PLD was delivered to virally-treated mice 8 days after virus injection. Control mice were treated with PBS. Tumor progression was monitored by bioluminescence imaging using the Xenogen IVIS Imaging System. Data points represent mean ± SD. (**c**) Kaplan–Meier survival plots were prepared and significance was determined using the log-rank method. *$P < 0.05$, **$P < 0.01$, ***$P < 0.001$. (**d**) Metastatic dissemination in the omentum, diaphragm, mesentery and peritoneal wall was assessed by identifying metastatic colonies (>5 mm) in individual mice at the time of development of bloody ascites in control mice. Representative images of metastasis within the peritoneal cavity of one mouse from each group are shown. OVV, oncolytic vaccinia virus; PBS, phosphate buffered saline; PFU, plaque forming units; PLD, pegylated liposomal doxorubicin; SD, standard deviation.

5b,c). In ID8-R tumor-bearing mice receiving the combined treatment with the armed virus, tumor growth was localized primarily in the omentum with only sporadic metastatic nodules (>5 mm) present in the peritoneal cavity (Figure 5d). The metastatic spread of the tumor was more prominent after OVV-Fc than the OVV-CXCR4-A-Fc treatment. In contrast, the control mice or those treated with PLD had metastatic nodules present on the omentum, mesentery, diaphragm, and peritoneal wall.

OVV-CXCR4-A-Fc followed by PLD inhibits tumor-immunosuppressive networks and induces antitumor CD8⁺ T cell responses

Previous studies have shown that virally-delivered CXCR4 antagonist can block the CXCL12/CXCR4 axis involved in tumor progression via enhanced local immunosuppression.[35,36,40] Therefore, we next investigated the effect of the single and combination treatments on intratumoral accumulation of neutrophils/granulocytic myeloid-derived suppressor cells (G-MDSCs) and Tregs[29,36] within the TME. The analysis performed on day 8 after completion of treatments revealed that the inhibition of tumor growth in ID8-R-bearing mice was associated with reduction of intraperitoneal recruitment of G-MDSCs ($CD11^+Ly6G^{high}Ly6C^{low}$) and Tregs ($CD4^+CD25^+Foxp3^+$) (Figure 6a,b). Strikingly, the combination treatment resulted in increased frequencies of $CD11c^+CD86^+$ DCs and IL-12-producing $CD11b^+F4/80^+$ inflammatory monocytes/macrophages in the peritoneal fluids of tumor-bearing mice (Figure 6c). These changes were associated with higher ratios of IFN-γ-producing $CD8^+$ to Tregs in the tumor-bearing animals treated with OVV-Fc or OVV-CXCR4-A-Fc followed by PLD as well as the presence of infiltrating tumor-specific $CD8^+$ T cells specific for the Wilms' tumor antigen 1 (WT1), a clinically relevant antigen target[41] expressed by ID8-R cells (Figure 6d–f). We then adoptively transferred 2×10^7 splenocytes from tumor-free mice with detectable WT1-specific T cell responses to ID8-R-bearing mice after combining them with LPS-matured $WT1_{126-134}$ peptide-pulsed BM-derived DCs.[42] Mice receiving splenocytes from animals with WT1-specific T cell responses showed reduced tumor growth

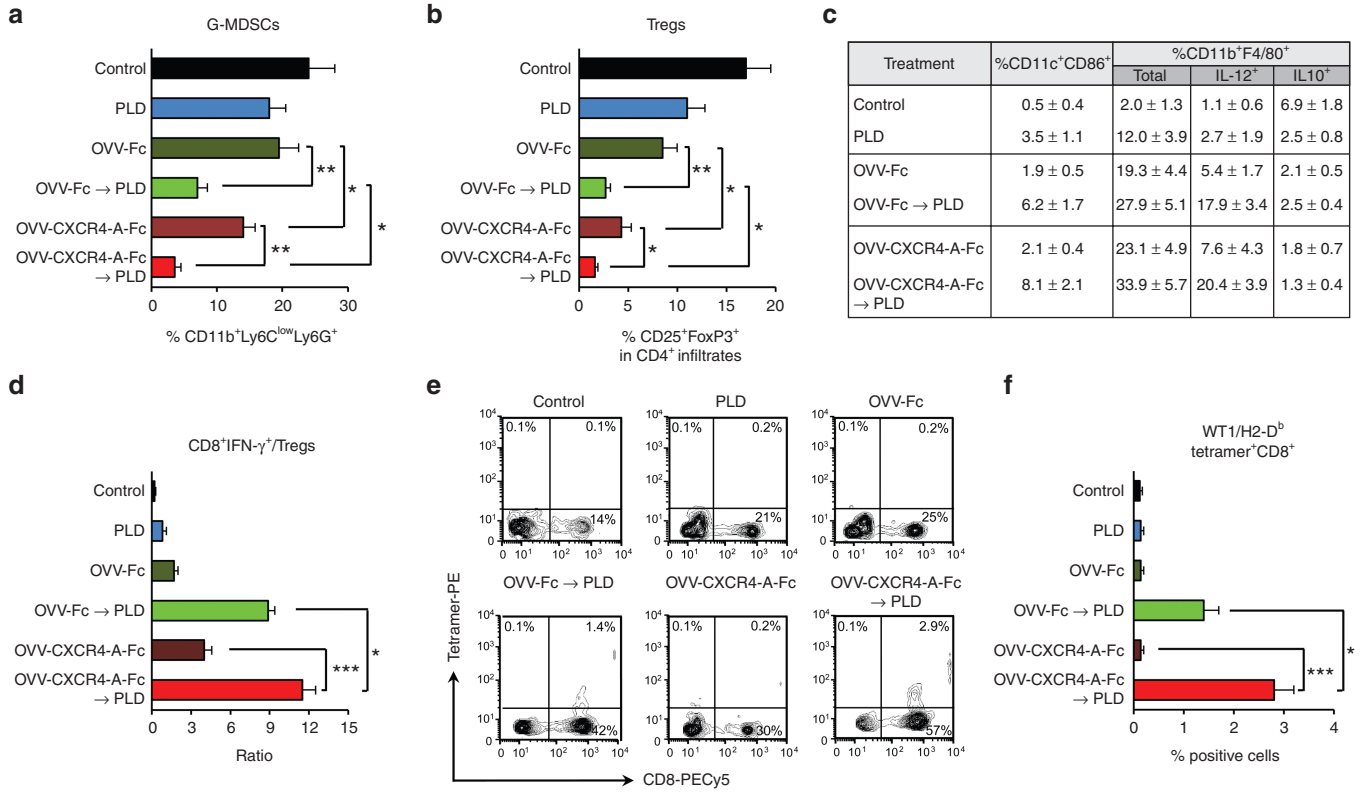

Treatment	%CD11c$^+$CD86$^+$	%CD11b$^+$F4/80$^+$		
		Total	IL-12$^+$	IL10$^+$
Control	0.5 ± 0.4	2.0 ± 1.3	1.1 ± 0.6	6.9 ± 1.8
PLD	3.5 ± 1.1	12.0 ± 3.9	2.7 ± 1.9	2.5 ± 0.8
OVV-Fc	1.9 ± 0.5	19.3 ± 4.4	5.4 ± 1.7	2.1 ± 0.5
OVV-Fc → PLD	6.2 ± 1.7	27.9 ± 5.1	17.9 ± 3.4	2.5 ± 0.4
OVV-CXCR4-A-Fc	2.1 ± 0.4	23.1 ± 4.9	7.6 ± 4.3	1.8 ± 0.7
OVV-CXCR4-A-Fc → PLD	8.1 ± 2.1	33.9 ± 5.7	20.4 ± 3.9	1.3 ± 0.4

Figure 6 Evaluation of immune infiltrates in ascites-derived tumors or peritoneal washes by combination treatments. Frequencies of G-MDSCs (CD11b$^+$Ly6C^{low}Ly6G$^+$) (**a**) Tregs (CD4$^+$CD25$^+$Foxp3$^+$) (**b**) in ascites-derived tumors of control and treated mice were analyzed by flow cytometry as described in the "Materials and Methods" section. Results are presented as mean ± SD of five mice per group. *P < 0.05, **P < 0.01. (**c**) The percent of CD11c$^+$CD86$^+$ DCs and CD11b$^+$F4/80$^+$ monocytes/macrophages in ascites derived tumors of the same groups of mice as above were analyzed by flow cytometry. The expression of IL-12 and IL-10 in CD11b$^+$F4/80$^+$ cells was determined by intracellular staining. Data points represent mean ± SD. (**d**) The ratios of IFN-γ-expressing CD8$^+$ T cells/Tregs in ascites-derived tumors were determined by intracellular staining with mAbs against IFN-γ-PE and CD8-PECy5 together with mAbs against Tregs (CD4$^+$CD25$^+$Foxp3$^+$) and flow cytometry of five mice per group. Data points represent mean ± SD. *P < 0.05, ***P < 0.001. (**e**) The percent of WT1$_{126\text{-}134}$ tetramer-specific CD8$^+$ T cells was determined by staining with anti-CD8-PECy5 mAb and PE-labeled H-2D^b-restricted WT1$_{126\text{-}134}$ tetramer. Background staining was assessed using isotype control antibodies. One representative experiment of five mice per group performed is shown. (**f**) Results are presented as mean ± SD of five mice per group. *P < 0.05, ***P < 0.001. IL-12, interluekin-12; IFN, interferon; SD, standard deviation.

compared with control mice, indicating the ability of the combined OVV-CXCR4-A-Fc and PDL treatment to promote the generation of durable antitumor immune responses (Supplementary Figure S8). Similarly, tumor-free survival was observed in 10% and 50% of CAOV2-R-bearing SCID mice treated with OVV-Fc and PLD and OVV-CXCR4-A-Fc and PLD, respectively (Supplementary Figure S9a,b). These results could be attributed to longer duration of productive viral replication/oncolysis in SCID mice and a direct effect of the CXCR4 antagonist on tumor cells as well as complement-dependent and antibody-dependent cell-mediated cytotoxicities.[29]

DISCUSSION

Cancer cells, with a high propensity for mutation, allow drug-resistant clones to emerge in tumors after anticancer drug therapy. This process, combined with the ability of tumors to influence their microenvironment by subverting stromal cells, culminate in treatment resistance, tumor relapse, and therapy failure,[43] suggesting that treatment strategies that can engage the patients' immune defense mechanisms through induction of ICD are important in contemporary cancer therapy. The approval of PLD in 1999, the recent FDA-approval of talimogene laherparepvec (T-VEC) virotherapy, and the ongoing clinical trial NCT02759588 of GL-ONC1 vaccinia virus against platinum-resistant and refractory ovarian cancers, all indicate we are entering a phase where these agents may significantly boost the armamentarium for cancer treatment. Importantly it is clear that platinum-resistant tumors become resistant to PLD used as a second line of treatment.[44] Also, oncolytic viruses are eliminated through induction of antiviral immune responses. Therefore, an effective combination treatment requires a well-coordinated strategy that would (i) synergistically augment tumor cell killing with simultaneous induction of ICD, (ii) reduce intratumoral recruitment of immunosuppressive elements in favor of immunostimulatory signals (*i.e.*, IL-12), and (iii) enhance local tumor-specific T cell accumulation to overcome a non-T-cell-inflamed TME to induce potent and durable antitumor immune responses. Here, we have demonstrated that ICD-inducing combination treatment consisting of OVV-CXCR4-A-Fc followed by PLD in PTX- and CBDCA-resistant ovarian tumor-bearing syngeneic mice significantly increased overall survival compared with single treatment modalities and reversed the immunosuppressive phenotype of the TME while promoting antitumor immunity.

Vaccinia virus can be considered as a suitable oncolytic virus candidate for treatment of drug-resistant ovarian tumors owing to its ability to infect a broad range of cells including CICs,[36,45] a rapid replication cycle, production of extracellular enveloped virions that evade the immune response,[46] and a capacity to spread to distant metastases following local delivery.[47] However, replication of the virus in CD44-expressing drug-resistant variants has not been

systematically explored and the mechanisms by which viral infection and replication is increased in resistant cells are still unclear. Vaccinia entry into target cells is thought to be mediated by glycosaminoglycans such as cell surface heparan sulfate that interacts with A27L viral membrane protein involved in a fusion of the virus to infected cells.[48,49] As isoforms of CD44 are differentially modified by glycosaminoglycans including heparan sulfate, chondroitin sulfate, and dermatan sulfate,[50,51] this suggests that higher expression of CD44 on the resistant variants could contribute to enhanced vaccinia infection, which is consistent with our findings. Furthermore, binding of CD44 to its cognate ligand hyaluronan initiates activation of several receptor tyrosine kinases, nonreceptor tyrosine kinases (SRC (Src)), and cytoskeleton linker proteins (reviewed in ref. [51]). This complex cross-talk results in activation of PI3K-Akt and ERK that correlates with tumor progression and drug resistance,[51,52] which are also known to augment vaccinia replication.[24,25] These latter findings are supported by at least 10-fold higher viral yields following infection of tumorigenic HeLa cells than those obtained following infection of embryo fibroblasts[25] and requirements of the MEK/ERK pathway for maximal vaccinia replication during productive infection in permissive cells, as both pharmacological and genetic inhibition of MEK/ERK resulted in decreases in viral yield.[24,53] In addition, the observed downregulation of CD44 expression in ID8-R-infected cells suggests a direct interaction between CD44 and vaccinia (data not shown), and studies are in progress to explore these interactions in drug-resistant clinical specimens derived from patients with epithelial ovarian cancer.

The finding that a synergistic interaction of vaccinia with DOX occurred in both murine and human PTX- and CBDCA-resistant ovarian cancer cell lines implies that common pathways may mediate the effect. Our results differed from those of Siurala *et al*., reporting DOX-mediated increases in adenoviral replication in human and hamster soft-tissue sarcoma cells.[20] In our studies, DOX inhibited OVV-mediated killing when added before the virus. This could be related to the ability of anthracyclines to stimulate the rapid production of Type 1 IFNs,[19] which in turn upregulates a large number of IFN-stimulated genes (*ISGs*)[54] with antiviral activities, including Myxovirus resistance (*MX*) genes (reviewed in ref. [55]). Therefore, the current findings suggest that ordering of OVV/DOX combination treatments may be specific to the selected virus, the chemosensitivity profile, and/or phenotype of the targeted tumor cells. An exogenous supply of Type 1 IFNs was also shown to restore the chemotherapeutic responses to DOX in *Tlr3*$^{-/-}$ but not *Ifnar2*$^{-/-}$ sarcomas growing in mice,[19] which was associated with robust *MX1* expression, consistent with improved chemotherapeutic responses to anthracyclines in patients with breast cancer who have poor prognosis.[19] Thus, the vaccinia-induced IFN-β in tumor cultures could explain the augmented responses to DOX characterized by higher expression of CRT and phagocytosis of tumor cell debris by DCs. The latter events are also necessary for complete DC activation and CD8^{+} T cell priming against tumor antigens.[56–58] Although the exposure of CRT on the cell surface of tumor cells is an important factor in determining immunogenicity of dying tumor cells,[59,60] a still-unresolved issue surrounding tumor growth involves the role that the immune system plays in resisting or eradicating the formation and progression of tumors.[43] During this process, cancer cells may paralyze infiltrating CTLs by secreting immunosuppressive factors[61] or by more subtle mechanisms that operate through the recruitment of immunosuppressive elements, including MDSCs and Tregs. The finding that combined CXCR4 antagonist-expressing virus and PLD inhibited intratumoral recruitment of MDSCs and Tregs while inducing antitumor immunity and tumor-free survival supports the latter argument. It is noteworthy that the ID8-R variants have been generated from parental tumor cells, which were recovered from syngeneic recipients. Herein, many distinct mechanisms of tumor cell escape from the immune system could contribute to outgrowth of the tumor mass, which may then display an altered cell phenotype.[62] Therefore, the ability of ID8-R tumor cells to generate spontaneous WT1-specific immune responses after treatment with OVV-CXCR4-A-Fc and PLD raises the possibility that the combination treatment with the armed oncolytic virotherapy and PLD rendered the tumor cells immunogenic by treatment-induced ICD while the suppressive elements in the tumor stroma have been compromised through our interventions. Alternatively, it is also conceivable that the *in vivo* selection process altered an immunogenic phenotype of the drug-resistant variants by changing expression levels of some tumor-associated antigens.

In conclusion, we have demonstrated that vaccinia virus expressing the CXCR4 antagonist synergizes with DOX in killing PTX- and CBDCA-resistant variants of ovarian cancer and inhibits metastatic spread of the tumor by reducing tumor load and induction of antitumor immune responses as depicted in Figure 7. The challenge for future investigation is to apply this strategy to the treatment of platinum-resistant or refractory human ovarian carcinomas in order to determine whether this combination can both engage the patient's immune system to promote *de novo* antitumor immune responses as well as to augment existing antitumor immunity.

MATERIALS AND METHODS

Animals and cell lines

Female C57BL/6 and C.B-Igh-1b/IcrTac-Prkdc SCID mice, 6–8 weeks of age were obtained from Charles River (Wilmington, MA) and the Laboratory of Animal Resources at Roswell Park Cancer Institute (RPCI), Buffalo, NY, respectively. Experimental procedures were performed in compliance with protocols approved by the Institutional Animal Care and Use Committee of the RPCI. The parental ID8 mouse ovarian epithelial cells derived from spontaneous malignant transformation of C57BL/6 MOSE cells.[63] The parental CAOV2 cell line was obtained from a collection maintained by the RPCI Department of Gynecologic Oncology. The genetic authenticity of CAOV2 cells was determined using microsatellite marker analysis[64] and the methylation status of the insulator protein CTCF within the insulin-like growth factor-II/H19 imprint center.[65] The drug-resistant ID8-R and CAOV2-R variants were generated by isolating tumor cells from ascites of tumor-bearing syngeneic and SCID mice, respectively, which had been challenged with pFU-Luc2-Tomato lentiviral vector-transduced ID8-T and CAOV2 tumors[36] and treated daily with 35 µmol/kg of PTX delivered i.p. for a period of 1 week. Subsequently, the tumor variants were cultured in the presence of PTX (35.4 nmol/l for ID8 and 118 nmol/l for CAOV2) for 3 months until they gained a PTX-resistant phenotype. Interestingly, the PTX-resistant variants also acquired cross-resistance to CBDCA (2.6 µmol/l). Then, both cell lines were maintained in culture media supplemented with 59 nmol/l PTX and 2.6 µmol/l CBDCA, resulting in ID8-R and CAOV2-R variants. Human HuTK^{-} 143 fibroblasts, human cervical carcinoma HeLa cells, and African green monkey cell line CV-1 were obtained from the American Type Culture Collection (Manassas, VA).

Viruses

All vaccinia viruses used in this study are of the Western Reserve strain with disrupted thymidine kinase and vaccinia growth factor genes for enhanced cancer cell specificity. The generation and characterization of OVVs expressing the EGFP, Fc portion of murine IgG2a and the CXCR4 antagonist consisting of the eight amino acids corresponding to the N-terminal sequence of CXCL12 with modified P to G (KGVSLSYR) expressed in the context of murine (Fc) or human (hFc) fragment of IgG with disulfide bonds in a hinge region for preservation of a dimeric structure present in the CTCE-9908 template (KGVSLSYR-K-RYSLSVGK)[39] have been described.[29,36]

Cytotoxicity assays

Cells plated in 96-well plates were infected with serial dilutions of OVV-EGFP, OVV-Fc or treated with increasing doses of DOX (Sigma Aldrich, St.

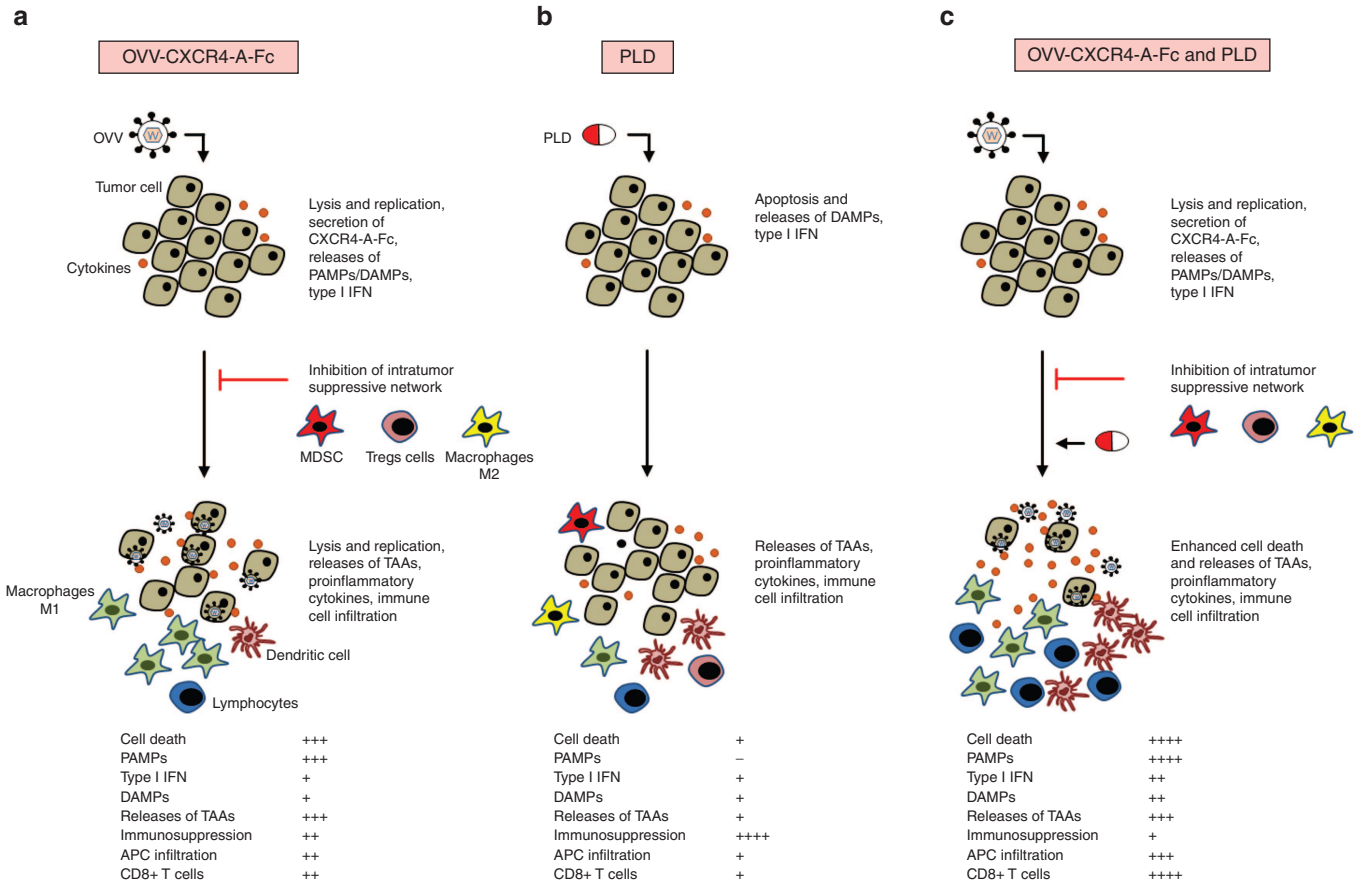

Figure 7 Graphical summary of improved long-term tumor-free survival by treatment of drug-resistant ovarian tumors *in vivo* by oncolytic virotherapy followed by PLD. (**a**) Intraperitoneal injection with OVV-CXCR4-A-Fc stimulates anticancer immunity through CXCR4-A-Fc-mediated inhibition of immunosuppressive cell recruitment, releases of pathogen-associated molecular patterns (PAMPs) and damage-associated molecular patterns (DAMPs) and immune cell infiltration, while also causing direct cellular cytotoxicity. (**b**) Treatment with PLD inhibits tumor growth through induction of immunogenic cell death, weakly effective in the drug-resistant mutants. (**c**) The synergistic interaction of OVV with PLD augments tumor cell death and inflammation, thus potentially increasing immunogenicity of endogenous tumor-associated antigens (TAAs). Low responses (+), medium responses (++), high responses (+++). OVV, oncolytic vaccinia virus; PLD, pegylated liposomal doxorubicin.

Louis, MO). For combination treatments, DOX was added at serial dilutions 12 hours after viral infection, together with the virus, or 12 hours before the infection. Cell survival was determined by 3-(4, 5-Dimethylthiazol-2-yl)-2, 5-diphenyltetrazolium bromide (MTT; Sigma) assays after 48 hours as described.[45] Cell survival was calculated using the following formula: % cell survival = (absorbance value of treated cells / absorbance value of untreated control cells) × 100%.

Viral replication

Tumor cells seeded into six-well plates were infected with OVV-EGFP at MOI = 1 and incubated at 37°C for 2 hours. Then, the infection medium was removed and cells were incubated in fresh medium until cell harvest at 24, 48, and 72 hours postinfection. In some experiments, DOX was added 12 hours after viral infection. Viral particles from the infected cells were released by performing a quick freeze-thaw cycle and the titer was determined by plaque assays on CV-1 cell monolayers and recorded as PFU/million cells. EGFP expression in virally-infected cultures was analyzed by flow cytometry or under fluorescent microscope (Zeiss Axiovert 40 CFL, 10×10) 24 hours after the infection.

Tumorigenicity assays and immunogenicity of dying tumor cells

Bulk cultures of parental and drug-resistant ID8 and CAOV2 tumor cells were injected i.p. using different numbers (5×10^4– 5×10^6) into either syngeneic C57BL/6 or SCID mice (n = 5–8) and monitored for tumor growth. To determine immunogenicity of dying tumor cells, 10^6 treated ID8-R cells were inoculated subcutaneously (s.c.) in 100 µl of phosphate buffered saline (PBS) into one flank of C57BL/6 six-week-old female mice, and 10^6 untreated control cells were inoculated into the opposite flank 8 days later. Tumor growth was monitored by measuring s.c. tumors with a microcaliper and determining tumor volume (width × length × width / 2 = mm^3).

Western blotting

Cells were starved after reaching 80–90% of confluence when the medium was changed to 1% fetal bovine serum (FBS) and incubated for 12 hours. Cells were solubilized in lysis buffer (Cell Signaling Technology, Danvers, MA) and samples of 25 ìg of total protein, determined by Bradford assay were separated on 4–20% Mini-Protean TGX gels (Bio-Rad Laboratories, Hercules, CA), transferred on to nitrocellulose membranes and incubated overnight with primary Abs against phospho-Akt (Ser473), phospho-Akt (Thr308), phospho-ERK1/2 (Thr202/Tyr204), Akt, ERK1/2 or glyceraldehyde 3-phosphate dehydrogenase (GAPDH) (Cell Signaling Technology). Bands were developed with horse radish peroxide (HRP)-labeled secondary Abs followed by Clarity Western ECL detection system (Bio-Rad Laboratories). Signal quantification was performed by densitometry analysis using a ChemiDoc MP imager and Image Lab software version 5.2.1 (Bio-Rad Laboratories).

The effect of DOX on expression of vaccinia virus antigens in infected cultures (MOI = 10) was analyzed 24 hours after the treatment. Cell lysates (25 µg/sample) were separated by sodium dodecyl sulfate (SDS)/polyacrylamide gel electrophoresis (PAGE) (10% gel), transferred on to nitrocellulose membranes, and incubated for 2 hours with OVV-specific mouse antiserum (1:2,000 dilution), prepared by immunizing C57BL/6 mice three times with 10^8 PFU of OVV-Fc, or normal mouse serum as control. After washing, the membranes were incubated with HRP-labeled secondary antibody.

Preparation of media collected from virally-infected cells (CVN media)

Tumor cells were infected with OVV-EGFP at MOI of 1, and media collected 24 hours later were filtered and treated with UV light (365 nm for 3 minutes) in the presence of 10 µg/ml psolaren to inactivate the virus.[66] A plaque assay was used to confirm lack of viral replication. Medium collected from uninfected cultures was used as a control. In some experiments, IFN-β levels in culture media were measured by ELISA (R&D Systems, Minneapolis, MN) according to the manufacturer's protocol.

Generation of BM-derived DC and *in vitro* phagocytosis assays

BM cells were flushed from the tibias and femurs of C57BL/6 mice with culture medium composed of Roswell Park Memorial Institute (RPMI) 1640 medium supplemented with 10% heat-inactivated fetal calf serum (FCS; Invitrogen, Carlsbad, CA), sodium pyruvate, 50 µmol/l 2-mercaptoethanol (Sigma), 10 mmol/l *N*-2-hydroxyethylpiperazine-*N9-2*-ethanesufonic acid (HEPES) (pH 7.4), and penicillin/streptomycin (Invitrogen). After one centrifugation, BM cells were resuspended in Tris-ammonium chloride for 2 minutes to lyse red blood cells. After one more centrifugation, BM cells (1×10^6 cells/ml) were cultured in medium supplemented with 10 ng/ml GM-CSF at 37°C for 6 days. The medium was replenished every 2–3 days. After 7 days, the nonadherent and loosely adherent cells were harvested, washed, and cocultured with cell tracker-blue CMF_2HC (Thermo Fisher Scientific, Grand Island, NY)-labeled tumor cells (1:1 ratio) for 12 hours. At the end of the incubation, cells were harvested with versene, pooled with nonadherent cells present in the supernatant, washed and stained with CD11c-APC antibody. Phagocytosis was assessed by fluorescence-activated cell sorting (FACS) analysis of double positive cells.

Treatment of established tumors

C57BL/6 mice ($n = 6$–10) were injected i.p. with 2×10^5 ID8-R cells, whereas SCID mice ($n = 6$) were injected i.p. with 2×10^6 CAOV2-R cells. Treatment with OVV-CXCR4-A-Fc or OVV-Fc (10^8 PFU delivered i.p.) was initiated 10 days later. In parallel experiments, tumor-bearing mice were treated with PLD alone (10 mg/kg, delivered i.v.) or PLD combined with OVV (delivered 8 days before, simultaneously of after virus injection). Tumor progression was monitored by bioluminescence imaging using the Xenogen IVIS Imaging System (PerkinElmer, Waltham, MA) after i.p. injection of 200 µl of Luciferin-D (150 mg/kg, Biosynth International, Itasca, IL). For experiments in CAOV2-R-challenged SCID mice, animals were treated with lower titers of the virus (2.5×10^7 PFU) and concentrations of PLD (5 mg/kg). Control mice received PBS or UV-inactivated virus. At the end of the experimental period corresponding to the development of bloody ascites in control mice, the tumor-bearing mice were sacrificed and organs were examined for tumor development and metastatic spread. Tumor and stromal cells were obtained from centrifuged cell pellets of ascites or peritoneal fluids collected from tumor-bearing mice after injection of 1 ml of PBS.

For adoptive transfer studies, C57BL/6 mice were injected s.c. with 10^5 ID8-R tumor cells and treated 10 days later (tumor volume ~100 mm^3) by i.v. injection of 2×10^7 splenocytes from tumor-bearing control mice or tumor-free mice with detectable WT1-specific immune responses after treatment with the OVV-CXCR4-A-Fc and PLD combination. Before the adoptive transfer, splenocytes were combined with LPS-matured $WT1_{126\text{-}134}$ peptide-pulsed BM-derived DCs (20:1) ratio as described.[42] Tumor growth was monitored by measuring s.c. tumors once to thrice a week with a microcaliper and determining tumor volume (width × length × width / 2 = mm^3).

Flow cytometry

Parental and drug-resistant ID8 tumor cells were analyzed by staining of single-cell suspensions with rat mAb against mouse CD44-PerCP-Cy5.5, whereas human CAOV2 tumor cells and their resistant variants were stained with mouse mAb against human CD44-PE (BD Pharmingen, San Jose, CA). The expression of CXCR4 on the surface of tumor cells was analyzed with rat mAb against mouse CXCR4-APC (BD Pharmingen) or human CXCR4-APC (eBioscience, San Diego, CA). The induction of apoptosis/necrosis in the resistant tumor cells treated with OVV-Fc (MOI = 1), DOX (1 µmol/l) alone or in combinations was assessed by staining with Annexin V-FITC and LIVE/DEAD fixable violet (Thermo Fisher Scientific) according to manufacturer's instruction. In some experiments, induction of apoptosis/necrosis was analyzed after incubating the resistant tumor cells for 24 hours with the CXCR4-A-Fc fusion proteins (100 µg/ml) isolated from culture supernatant of infected cells by protein G column as described.[29] Cultures incubated with the Fc portion of murine IgG2a served as control. Tumor cells were analyzed for cell surface expression of ecto-CRT by staining with rabbit anti-mouse CRT mAb (Abcam, Cambridge, MA) followed by staining with APC-conjugated goat antirabbit secondary antibody (Santa Cruz Biotechnology, Santa Cruz, CA). The prevalence of SP cells in the parental and drug-resistant ID8 and CAOV2 cultures was determined on single-cell suspensions stained with Hoechst 33342 dye (Sigma) at a concentration of 5 µg/ml (37°C for 2 hours) as described.[27] Cell analysis was performed on a LRS II flow cytometer (BD Biosciences, San Jose, CA). After excitation of the Hoechst dye at 350 nm and measurement of the fluorescence profile in dual-wavelength analysis (405/30 nm and 670/40 nm), the SP was defined as described.[67]

The phenotypic analysis of G-MDSCs, Tregs, DCs, inflammatory monocytes/macrophages expressing IL-12 or IL-10, and $CD8^+$ T lymphocytes were performed on single-cell suspensions prepared from peritoneal fluids collected 8 days after all treatments. The cells were stained with rat mAbs against mouse CD11b-APC, Ly6G-PE, Ly6C-FITC, CD45-APC-Cy7, CD4-PECy5, CD25-FITC, CD8-PECy5, IFN-γ-PE, CD11c-APC, CD86-FITC (BD Pharmingen), and Foxp3-AlexaFluor 647 (eBioscience), and F4/80-FITC (BioLegend, San Diego, CA). Percentages of $CD8^+$ T cells expressing IFN-γ or $CD4^+$ T cells expressing Foxp3 were determined by intracellular staining using BD Pharmingen Transcription Factor Buffer Set (BD Biosciences) according to the manufacturer's protocol. Percentages of $CD11b/F4/80^+$ macrophages expressing IL-12 or IL-10 were determined by intracellular staining with rat mAb against mouse IL-10-PE (BD Pharmingen) and antih/m IL-12/ILp35-PE Ab (R&D Systems). To determine the percent of $WT1_{126\text{-}134}/H\text{-}2D^b$ tetramer-specific $CD8^+$ tumor-associated T lymphocytes, cells were stained with rat antimouse CD8-PECy5 mAb and a PE-labeled $WT1_{126\text{-}134}/H\text{-}2D^b$ tetramer (MHC Tetramer Production Facility, Baylor College of Medicine, Houston, TX). Immune cells were gated on $CD45^+$ viable cells for the analysis. For tetramer analysis, lymphocytes were also gated on cells that were negative for CD11b and Gr1 expression. Background staining was assessed using isotype control antibodies. Before specific antibody staining, cells were incubated with Fc blocker (anti-CD16/CD32 mAb) for 10 minutes followed by Live/Dead Fixable Violet Dead Cell stain kit (Thermo Fisher Scientific) to assess live/dead cells, and analyzed on a LRS II flow cytometer (BD Biosciences). Data analysis was performed using WinList 3D 7.1 (Verity Software House, Topsham, ME).

Statistical analysis

All statistical analyses were performed using GraphPad Prism 6 (GraphPad Software, La Jolla, CA). Unless otherwise noted, data are presented as mean ± SD (standard deviation), combined with unpaired, two-tailed Student's *t*-test. Kaplan–Meier survival plots were prepared and median survival times were determined for tumor-challenged groups of mice. Statistical differences in the survival across groups were assessed using the log-rank Mantel–Cox method. The threshold for statistical significance was set to $P < 0.05$.

CONFLICTS OF INTEREST

The authors declare no competing financial interest.

ACKNOWLEDGMENTS

We thank Michael F. Clarke for the pFU–Luc2–Tomato lentiviral vector, the Flow Cytometry Core and Laboratory Animal Resources for services and technical support. This work was supported in part by the National Institutes of Health grants CA164475 and Roswell Park Alliance Foundation (to D. Kozbor); the NCI-funded RPCI-UPCI Ovarian Cancer SPORE P50CA159981 (to K. Odunsi and D. Kozbor); and the NIH Cancer Center Support Grant, P30 CA016056 (to C. Johnson and K. Odunsi). M.P.K., A.J.R.M., A.K., and M.G. performed the experiments; M.J.N., M.O., K.O.O., K.E., and B.L. designed, performed data analysis and manuscript review; D.K. designed the experiments, analyzed, and interpreted the data. M.P.K. and D.K. drafted the manuscript.

REFERENCES

1. Bast, RC Jr, Hennessy, B and Mills, GB (2009). The biology of ovarian cancer: new opportunities for translation. *Nat Rev Cancer* **9**: 415–428.
2. Jemal, A, Siegel, R, Ward, E, Hao, Y, Xu, J and Thun, MJ (2009). Cancer statistics, 2009. *CA Cancer J Clin* **59**: 225–249.

3. Thigpen, JT, Blessing, JA, Ball, H, Hummel, SJ and Barrett, RJ (1994). Phase II trial of paclitaxel in patients with progressive ovarian carcinoma after platinum-based chemotherapy: a Gynecologic Oncology Group study. *J Clin Oncol* **12**: 1748–1753.
4. Huang, EH, Heidt, DG, Li, CW and Simeone, DM (2007). Cancer stem cells: a new paradigm for understanding tumor progression and therapeutic resistance. *Surgery* **141**: 415–419.
5. Alvero, AB, Chen, R, Fu, HH, Montagna, M, Schwartz, PE, Rutherford, T *et al.* (2009). Molecular phenotyping of human ovarian cancer stem cells unravels the mechanisms for repair and chemoresistance. *Cell Cycle* **8**: 158–166.
6. Dean, M, Fojo, T and Bates, S (2005). Tumor stem cells and drug resistance. *Nat Rev Cancer* **5**: 275–284.
7. Craveiro, V, Yang-Hartwich, Y, Holmberg, JC, Joo, WD, Sumi, NJ, Pizzonia, J *et al.* (2013). Phenotypic modifications in ovarian cancer stem cells following Paclitaxel treatment. *Cancer Med* **2**: 751–762.
8. Sato, E, Olson, SH, Ahn, J, Bundy, B, Nishikawa, H, Qian, F *et al.* (2005). Intraepithelial CD8+ tumor-infiltrating lymphocytes and a high CD8+/regulatory T cell ratio are associated with favorable prognosis in ovarian cancer. *Proc Natl Acad Sci USA* **102**: 18538–18543.
9. Odunsi, K, Qian, F, Matsuzaki, J, Mhawech-Fauceglia, P, Andrews, C, Hoffman, EW *et al.* (2007). Vaccination with an NY-ESO-1 peptide of HLA class I/II specificities induces integrated humoral and T cell responses in ovarian cancer. *Proc Natl Acad Sci USA* **104**: 12837–12842.
10. Hwang, WT, Adams, SF, Tahirovic, E, Hagemann, IS and Coukos, G (2012). Prognostic significance of tumor-infiltrating T cells in ovarian cancer: a meta-analysis. *Gynecol Oncol* **124**: 192–198.
11. Lichty, BD, Breitbach, CJ, Stojdl, DF and Bell, JC (2014). Going viral with cancer immunotherapy. *Nat Rev Cancer* **14**: 559–567.
12. Workenhe, ST, Simmons, G, Pol, JG, Lichty, BD, Halford, WP and Mossman, KL (2014). Immunogenic HSV-mediated oncolysis shapes the antitumor immune response and contributes to therapeutic efficacy. *Mol Ther* **22**: 123–131.
13. Unterholzner, L, Keating, SE, Baran, M, Horan, KA, Jensen, SB, Sharma, S *et al.* (2010). IFI16 is an innate immune sensor for intracellular DNA. *Nat Immunol* **11**: 997–1004.
14. Myskiw, C, Arsenio, J, Booy, EP, Hammett, C, Deschambault, Y, Gibson, SB *et al.* (2011). RNA species generated in vaccinia virus infected cells activate cell type-specific MDA5 or RIG-I dependent interferon gene transcription and PKR dependent apoptosis. *Virology* **413**: 183–193.
15. Duda, DG, Kozin, SV, Kirkpatrick, ND, Xu, L, Fukumura, D and Jain, RK (2011). CXCL12 (SDF1alpha)-CXCR4/CXCR7 pathway inhibition: an emerging sensitizer for anticancer therapies? *Clin Cancer Res* **17**: 2074–2080.
16. Teicher, BA (2011). Antiangiogenic agents and targets: A perspective. *Biochem Pharmacol* **81**: 6–12.
17. Pisano, C, Cecere, SC, Di Napoli, M, Cavaliere, C, Tambaro, R, Facchini, G *et al.* (2013). Clinical trials with pegylated liposomal Doxorubicin in the treatment of ovarian cancer. *J Drug Deliv* **2013**: 898146.
18. Woo, SR, Corrales, L and Gajewski, TF (2015). The STING pathway and the T cell-inflamed tumor microenvironment. *Trends Immunol* **36**: 250–256.
19. Sistigu, A, Yamazaki, T, Vacchelli, E, Chaba, K, Enot, DP, Adam, J *et al.* (2014). Cancer cell-autonomous contribution of type I interferon signaling to the efficacy of chemotherapy. *Nat Med* **20**: 1301–1309.
20. Siurala, M, Bramante, S, Vassilev, L, Hirvinen, M, Parviainen, S, Tähtinen, S *et al.* (2015). Oncolytic adenovirus and doxorubicin-based chemotherapy results in synergistic antitumor activity against soft-tissue sarcoma. *Int J Cancer* **136**: 945–954.
21. Zhang, S, Balch, C, Chan, MW, Lai, HC, Matei, D, Schilder, JM *et al.* (2008). Identification and characterization of ovarian cancer-initiating cells from primary human tumors. *Cancer Res* **68**: 4311–4320.
22. Cioffi, M, D'Alterio, C, Camerlingo, R, Tirino, V, Consales, C, Riccio, A *et al.* (2015). Identification of a distinct population of CD133(+)CXCR4(+) cancer stem cells in ovarian cancer. *Sci Rep* **5**: 10357.
23. Wang, G, Barrett, JW, Stanford, M, Werden, SJ, Johnston, JB, Gao, X *et al.* (2006). Infection of human cancer cells with myxoma virus requires Akt activation via interaction with a viral ankyrin-repeat host range factor. *Proc Natl Acad Sci USA* **103**: 4640–4645.
24. Andrade, AA, Silva, PN, Pereira, AC, De Sousa, LP, Ferreira, PC, Gazzinelli, RT *et al.* (2004). The vaccinia virus-stimulated mitogen-activated protein kinase (MAPK) pathway is required for virus multiplication. *Biochem J* **381** (Pt 2): 437–446.
25. Soares, JA, Leite, FG, Andrade, LG, Torres, AA, De Sousa, LP, Barcelos, LS *et al.* (2009). Activation of the PI3K/Akt pathway early during vaccinia and cowpox virus infections is required for both host survival and viral replication. *J Virol* **83**: 6883–6899.
26. Hirschmann-Jax, C, Foster, AE, Wulf, GG, Goodell, MA and Brenner, MK (2005). A distinct "side population" of cells in human tumor cells: implications for tumor biology and therapy. *Cell Cycle* **4**: 203–205.
27. Hirschmann-Jax, C, Foster, AE, Wulf, GG, Nuchtern, JG, Jax, TW, Gobel, U *et al.* (2004). A distinct "side population" of cells with high drug efflux capacity in human tumor cells. *Proc Natl Acad Sci USA* **101**: 14228–14233.
28. Stripecke, R, Carmen Villacres, M, Skelton, D, Satake, N, Halene, S and Kohn, D (1999). Immune response to green fluorescent protein: implications for gene therapy. *Gene Ther* **6**: 1305–1312.
29. Gil, M, Seshadri, M, Komorowski, MP, Abrams, SI and Kozbor, D (2013). Targeting CXCL12/CXCR4 signaling with oncolytic virotherapy disrupts tumor vasculature and inhibits breast cancer metastases. *Proc Natl Acad Sci USA* **110**: E1291–E1300.
30. McCart, JA, Ward, JM, Lee, J, Hu, Y, Alexander, HR, Libutti, SK *et al.* (2001). Systemic cancer therapy with a tumor-selective vaccinia virus mutant lacking thymidine kinase and vaccinia growth factor genes. *Cancer Res* **61**: 8751–8757.
31. Kroemer, G, Galluzzi, L, Kepp, O and Zitvogel, L (2013). Immunogenic cell death in cancer therapy. *Annu Rev Immunol* **31**: 51–72.
32. Gardai, SJ, McPhillips, KA, Frasch, SC, Janssen, WJ, Starefeldt, A, Murphy-Ullrich, JE *et al.* (2005). Cell-surface calreticulin initiates clearance of viable or apoptotic cells through trans-activation of LRP on the phagocyte. *Cell* **123**: 321–334.
33. Ogden, CA, deCathelineau, A, Hoffmann, PR, Bratton, D, Ghebrehiwet, B, Fadok, VA *et al.* (2001). C1q and mannose binding lectin engagement of cell surface calreticulin and CD91 initiates macropinocytosis and uptake of apoptotic cells. *J Exp Med* **194**: 781–795.
34. Obeid, M, Panaretakis, T, Joza, N, Tufi, R, Tesniere, A, van Endert, P *et al.* (2007). Calreticulin exposure is required for the immunogenicity of gamma-irradiation and UVC light-induced apoptosis. *Cell Death Differ* **14**: 1848–1850.
35. Cojoc, M, Peitzsch, C, Trautmann, F, Polishchuk, L, Telegeev, GD and Dubrovska, A (2013). Emerging targets in cancer management: role of the CXCL12/CXCR4 axis. *Onco Targets Ther* **6**: 1347–1361.
36. Gil, M, Komorowski, MP, Seshadri, M, Rokita, H, McGray, AJ, Opyrchal, M *et al.* (2014). CXCL12/CXCR4 blockade by oncolytic virotherapy inhibits ovarian cancer growth by decreasing immunosuppression and targeting cancer-initiating cells. *J Immunol* **193**: 5327–5337.
37. Wong, D and Korz, W (2008). Translating an antagonist of chemokine receptor CXCR4: from bench to bedside. *Clin Cancer Res* **14**: 7975–7980.
38. Hotte, SJ, Hirte, HW, Moretto, P, Iacobucci, A, Wong, D, Korz, W *et al.* (2008). Final results of a phase I/II study of CTCE-9908, a novel anticancer agent that inhibits CXCR4, in patients with advanced solid cancers. [abstract 405] EORTC/NCI/AACR Molecular Targets and Cancer Therapeutics 2008 conference; October 2008. *Eur J Cancer* **6**: 127.
39. Huang, EH, Singh, B, Cristofanilli, M, Gelovani, J, Wei, C, Vincent, L *et al.* (2009). *J Surg Res* **155**: 231–236.
40. Scotton, CJ, Wilson, JL, Scott, K, Stamp, G, Wilbanks, GD, Fricker, S *et al.* (2002). Multiple actions of the chemokine CXCL12 on epithelial tumor cells in human ovarian cancer. *Cancer Res* **62**: 5930–5938.
41. Hylander, B, Repasky, E, Shrikant, P, Intengan, M, Beck, A, Driscoll, D *et al.* (2006). Expression of Wilms tumor gene (WT1) in epithelial ovarian cancer. *Gynecol Oncol* **101**: 12–17.
42. Gil, M, Bieniasz, M, Wierzbicki, A, Bambach, BJ, Rokita, H and Kozbor, D (2009). Targeting a mimotope vaccine to activating Fcgamma receptors empowers dendritic cells to prime specific CD8+ T cell responses in tumor-bearing mice. *J Immunol* **183**: 6808–6818.
43. Hanahan, D and Weinberg, RA (2011). Hallmarks of cancer: the next generation. *Cell* **144**: 646–674.
44. Smith, L, Watson, MB, O'Kane, SL, Drew, PJ, Lind, MJ and Cawkwell, L (2006). The analysis of doxorubicin resistance in human breast cancer cells using antibody microarrays. *Mol Cancer Ther* **5**: 2115–2120.
45. Wang, H, Chen, NG, Minev, BR and Szalay, AA (2012). Oncolytic vaccinia virus GLV-1h68 strain shows enhanced replication in human breast cancer stem-like cells in comparison to breast cancer cells. *J Transl Med* **10**: 167.
46. Vanderplasschen, A, Mathew, E, Hollinshead, M, Sim, RB and Smith, GL (1998). Extracellular enveloped vaccinia virus is resistant to complement because of incorporation of host complement control proteins into its envelope. *Proc Natl Acad Sci USA* **95**: 7544–7549.
47. Park, BH, Hwang, T, Liu, TC, Sze, DY, Kim, JS, Kwon, HC *et al.* (2008). Use of a targeted oncolytic poxvirus, JX-594, in patients with refractory primary or metastatic liver cancer: a phase I trial. *Lancet Oncol* **9**: 533–542.
48. Chung, CS, Hsiao, JC, Chang, YS and Chang, W (1998). A27L protein mediates vaccinia virus interaction with cell surface heparan sulfate. *J Virol* **72**: 1577–1585.
49. Hsiao, JC, Chung, CS and Chang, W (1998). Cell surface proteoglycans are necessary for A27L protein-mediated cell fusion: identification of the N-terminal region of A27L protein as the glycosaminoglycan-binding domain. *J Virol* **72**: 8374–8379.
50. Greenfield, B, Wang, WC, Marquardt, H, Piepkorn, M, Wolff, EA, Aruffo, A *et al.* (1999). Characterization of the heparan sulfate and chondroitin sulfate assembly sites in CD44. *J Biol Chem* **274**: 2511–2517.
51. Misra, S, Hascall, VC, Markwald, RR and Ghatak, S (2015). Interactions between Hyaluronan and its receptors (CD44, RHAMM) regulate the activities of inflammation and cancer. *Front Immunol* **6**: 201.
52. Testa, JR and Bellacosa, A (2001). AKT plays a central role in tumorigenesis. *Proc Natl Acad Sci USA* **98**: 10983–10985.
53. Silva, PN, Soares, JA, Brasil, BS, Nogueira, SV, Andrade, AA, de Magalhães, JC *et al.* (2006). Differential role played by the MEK/ERK/EGR-1 pathway in orthopoxviruses vaccinia and cowpox biology. *Biochem J* **398**: 83–95.
54. Der, SD, Zhou, A, Williams, BR and Silverman, RH (1998). Identification of genes differentially regulated by interferon alpha, beta, or gamma using oligonucleotide arrays. *Proc Natl Acad Sci USA* **95**: 15623–15628.

55. Melchjorsen, J (2013). Learning from the messengers: innate sensing of viruses and cytokine regulation of immunity—clues for treatments and vaccines. *Viruses* **5**: 470–527.
56. Gajewski, TF (2015). The next hurdle in cancer immunotherapy: overcoming the non-T-cell-inflamed tumor microenvironment. *Semin Oncol* **42**: 663–671.
57. Spranger, S, Bao, R and Gajewski, TF (2015). Melanoma-intrinsic β-catenin signalling prevents anti-tumour immunity. *Nature* **523**: 231–235.
58. Woo, SR, Corrales, L and Gajewski, TF (2015). Innate immune recognition of cancer. *Annu Rev Immunol* **33**: 445–474.
59. Obeid, M, Tesniere, A, Panaretakis, T, Tufi, R, Joza, N, van Endert, P *et al.* (2007). Ecto-calreticulin in immunogenic chemotherapy. *Immunol Rev* **220**: 22–34.
60. Obeid, M, Tesniere, A, Ghiringhelli, F, Fimia, GM, Apetoh, L, Perfettini, JL *et al.* (2007). Calreticulin exposure dictates the immunogenicity of cancer cell death. *Nat Med* **13**: 54–61.
61. Yang, L, Pang, Y and Moses, HL (2010). TGF-beta and immune cells: an important regulatory axis in the tumor microenvironment and progression. *Trends Immunol* **31**: 220–227.
62. Teng, MW, Swann, JB, Koebel, CM, Schreiber, RD and Smyth, MJ (2008). Immune-mediated dormancy: an equilibrium with cancer. *J Leukoc Biol* **84**: 988–993.
63. Janát-Amsbury, MM, Yockman, JW, Anderson, ML, Kieback, DG and Kim, SW (2006). Comparison of ID8 MOSE and VEGF-modified ID8 cell lines in an immunocompetent animal model for human ovarian cancer. *Anticancer Res* **26** (4B): 2785–2789.
64. Korch, C, Spillman, MA, Jackson, TA, Jacobsen, BM, Murphy, SK, Lessey, BA *et al.* (2012). DNA profiling analysis of endometrial and ovarian cell lines reveals misidentification, redundancy and contamination. *Gynecol Oncol* **127**: 241–248.
65. Huang, Z and Murphy, SK (2013). Increased intragenic IGF2 methylation is associated with repression of insulator activity and elevated expression in serous ovarian carcinoma. *Front Oncol* **3**: 131.
66. Gil, M, Bieniasz, M, Seshadri, M, Fisher, D, Ciesielski, MJ, Chen, Y *et al.* (2011). Photodynamic therapy augments the efficacy of oncolytic vaccinia virus against primary and metastatic tumours in mice. *Br J Cancer* **105**: 1512–1521.
67. Goodell, MA, Brose, K, Paradis, G, Conner, AS and Mulligan, RC (1996). Isolation and functional properties of murine hematopoietic stem cells that are replicating *in vivo*. *J Exp Med* **183**: 1797–1806.

Supplementary Information accompanies this paper on the *Molecular Therapy—Oncolytics* website (http://www.nature.com/mto)